ACS APPLIED MATERIALS & INTERFACES

Research Article

www.acsami.org

# Deformation Hysteresis of Electrohydrodynamic Patterning on a Thin Polymer Film

Qingzhen Yang,[†,‡] Ben Q. Li,[∥] Hongmiao Tian,[§] Xiangming Li,[§] Jinyou Shao,[§] Xiaoliang Chen,[§] and Feng Xu*[,†,‡]

[†]The Key Laboratory of Biomedical Information Engineering of the Ministry of Education, School of Life Science and Technology, [‡]Bioinspired Engineering and Biomechanics Center (BEBC), and [§]State Key Laboratory for Manufacturing Systems Engineering, Xi'an Jiaotong University, Xi'an, Shaanxi 710049, People's Republic of China

[∥]Department of Mechanical Engineering, University of Michigan—Dearborn, Dearborn, Michigan 48128, United States

Supporting Information

**ABSTRACT:** Electrohydrodynamic patterning is a technique that enables micro/nanostructures via imposing an external voltage on thin polymer films. In this investigation, we studied the electrohydrodynamic patterning theoretically and experimentally, with special interest focused on the equilibrium state. It is found that the equilibrium structure height increases with the voltage. In addition, we have observed, and believe it to be the first time, a hysteresis phenomenon exists in the relationship between the voltage and structure height. With an increase in the voltage, a critical value (the first critical voltage) is noticed, above which the polymer film would increase dramatically until it comes into contact with the template. However, with a decrease in the voltage, a smaller voltage (the second critical voltage) is needed to detach the polymer from the template. The mismatch of the first and second critical voltages distorts the voltage−structure height curve into an "S" shape. Such a phenomenon is verified for three representative templates and also by experiments. Furthermore, the effects of some parameters (e.g., polymer film thickness and dielectric constant) on this hysteresis phenomenon are also discussed.

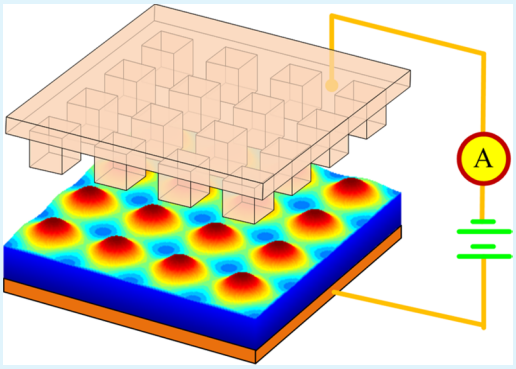


**KEYWORDS:** *micro/nanopatterning, polymer film, electrohydrodynamics, hysteresis phenomenon, numerical modeling*

## INTRODUCTION

With the development of integrated circuits,[1] energy storage,[2] and biotechnology,[3] high-definition micro/nanopatterns are in a real and urgent need. Numerous fabrication methods have been proposed.[4] Among them, electrohydrodynamic patterning is a technique that enables micro/nanostructures on thin polymer films and is being considered as an alternative to the conventional lithography.[5] In this method, a thin liquid polymer film is uniformly coated on a substrate (e.g., glass or silicon wafer). Then a conductive template with or without patterns is placed above the polymer film at a distance. After that, an electric voltage is applied between the substrate and template, and then the polymer film flows due to the action of the electric force. Eventually, the liquid polymer is transformed into a solid by photo- or thermocuring, leading to a micro/nanostructure. One major merit of such a method is that it could economically overcome the optical limit and scale down the structure to less than 100 nm.[6]

Electrohydrodynamic patterning emerged more than one decade ago and should be contributed to Chou[7,8] and Schaffer.[9] Extensive work has also been done by other researchers, and various micro/nanopatterns have been implemented. For the template without structures (i.e., flat), usually hexagonal distributed pillars are obtained.[5,10] For the template with structures, usually the polymer underneath a protrusion part grows upward, and due to the requirement of mass conservation, the rest of the polymer tends to fall down, leading to a positive replica of the template. This technique has found numerous applications in academia and industry, such as concave microlens arrays,[11] superhydrophobic surfaces,[12] and biomimic dry adhesive structures.[13]

In experiments, there appear to be some trends in the electrohydrodynamic patterning. The first one is to fabricate more complicated multilayer structures, such as polymer/polymer bilayer structures[14,15] and polymer/polymer/air[16] or polymer/air/polymer[17] trilayer structures. The second trend is to attempt to scale down the polymer structure and improve its height/width ratio.[18,19] Some methods are demonstrated to be effective, such as increasing the electrical permittivity of the polymer,[20] utilizing the conductive polymer,[21,22] and decreasing the surface tension coefficient.[23]

**Received:** April 8, 2016
**Accepted:** June 21, 2016

  

DOI: 10.1021/acsami.6b04192
*ACS Appl. Mater. Interfaces* XXXX, XXX, XXX−XXX

On the theoretical aspect, extensive work has also been conducted by researchers. As stated before, for the flat template, usually hexagonal distributed pillars are obtained on the film.[5,9] To predict the pillar diameter and the distance between two adjacent pillars, the most unstable wavelength has been derived using the linear stability analysis.[20,24] Regarding the structured template, most research focuses on the temporal evolution of the polymer film, and three different methods have been proposed thus far. The first one is a linear method which employs the long wave approximation and ignores all the linear terms.[25−28] Wu et al. then developed the second one, a weakly nonlinear method in which some nonlinear terms are considered.[29] The third one is a fully nonlinear method in which all the nonlinear terms are included, which thus makes it the most accurate. To be specific, the following models have been successfully used in simulating electrohydrodynamic patterning: phase field method,[30−34] moving mesh method,[35] and level set method.[36]

All these research efforts focus on the dynamic process of electrohydrodynamic patterning. Another important aspect is the steady state (or equilibrium state), which represents the ultimate state that the polymer film eventually evolves into.[37−40] In this paper, we shed light on the equilibrium state of the polymer film. A mathematical model based on the arc length continuation enhanced finite different method was developed, enabling the equilibrium deformation for a given external voltage. Extensive numerical simulations are performed for different voltages, and it is found that a hysteresis phenomenon occurs. To be specific, when the voltage is increased and decreased, different deformations are obtained for the same voltage. This hysteresis phenomenon is studied for different templates and different process parameters. Experiments are also conducted to verify such a hysteresis phenomenon.

## MATHEMATICAL FORMULATION

A representative configuration is illustrated in Figure 1a. A thin layer of polymer film with an initial thickness $h_0$ is coated on the substrate (i.e., lower electrode). A prestructured template is laid above the film with a distance $d_0$. Since the entire configuration is placed in the natural environment, air fills the gap. Both the polymer and air are considered as incompressible Newtonian fluids. The density, viscosity, and electrical permittivity of the fluid are represented by $\rho_i$, $\mu_i$, and $\varepsilon_i$, respectively ($i$ = 1 for air and 2 for the polymer). Both the air and polymer are considered as dielectric. The template and lower electrode are conductive; thus, after a voltage $U$ is imposed, the polymer film starts to deform due to the electric force.

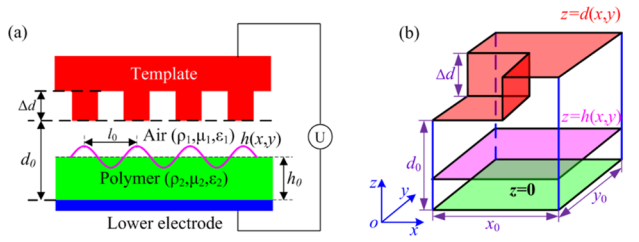


**Figure 1.** Schematic view of the electrohydrodynamic patterning: (a) configuration; (b) computational domain. The template could be in various shapes. The case shown here is a representative one.

The template could have different morphologies, without loss of generality. Figure 1b shows one representative case where the template is marked with square pillars. For such a case, the periodic length is denoted by $\lambda$ in each direction $x$ and $y$. Taking advantage of the periodicity and symmetricity, one-fourth of the periodic zone is chosen as the computational domain as shown in Figure 1b. $d(x, y)$ indicates the morphology of the template, and $h(x, y)$ denotes the polymer/air interface, which is the objective to solve. For differently shaped templates, the governing equations are essentially the same.

We developed a mathematical model to predict the polymer film deformation $h(x, y)$ for a given external voltage $U$. When the polymer film is in its equilibrium state, the forces are balanced along the polymer/air interface, which is expressed as (see the Supporting Information for the details)

$$\gamma\nabla^2 h + P_{gag} + \frac{1}{2}\varepsilon_0\left(\frac{1}{\varepsilon_1} - \frac{1}{\varepsilon_2}\right)\left[\frac{\varepsilon_1\varepsilon_2 U}{\varepsilon_1 h + \varepsilon_2(d-h)}\right]^2 + \left[\frac{A_L}{6\pi h^3} - \frac{A_U}{6\pi(d-h)^3}\right] = 0 \quad (1)$$

where $\gamma$ is the surface tension coefficient, $P_{gag}$ is a constant, $\varepsilon_0 = 8.85 \times 10^{-12}$ F/m is the permittivity of a vacuum, $\varepsilon_1$ ($\varepsilon_2$) is the dielectric constant of air (polymer), $d(x, y)$ indicates the morphology of the template, and $A_L$ ($A_U$) is the effective Hamaker constant for the lower (upper) electrode.[29,41] The first term in the above equation represents the surface tension force, the second one indicates the pressure difference inside/outside the polymer film, the third one denotes the electric force along the interface, and the last one is the Lifshitz−van der Waals (LW) force between the polymer and template and polymer and substrate.

## EXPERIMENTAL SECTION

**Methods.** We conducted a verification experiment to justify the hysteresis phenomenon in electrohydrodynamic patterning. As illustrated in Figure 1a, a thin layer of polymer film was first spin-coated onto an indium_ tin oxide (ITO)/glass substrate serving as one of the electrodes. Some metal needles were placed in a row and acted as another electrode. This needle array was laid above the polymer film with an air gap. To tune the air gap, the needle array was attached to a manual translation stage with a high resolution of 1 $\mu$m. In our experiments, the air gap could be tuned by moving the stage upward/downward. Once a dc voltage was imposed between the template (i.e., needle array) and the substrate (i.e., ITO), the polymer film moved upward to the template under the action of the electric force, leading to a microstructure. We maintained the voltage for a sufficiently long time (2 h) to ensure an equilibrium was achieved at such a voltage.

**Materials and Equipment.** The ITO glass was obtained by sputtering a thin layer of ITO onto a glass plate via a Denton Vacuum Explorer14 sputterer. The needles were commercially available and were purchased from Dongbang Inc. (Suzhou, China). In the experiments, we used a UV-curable polymer, OrmoStamp (from Micro Resist Technology, Germany), with the main component being acrylate. This polymer has a relative electrical permittivity of 6, a mass density of 960 kg/m$^3$, a viscosity of 0.34 Pa·s, and a surface tension of 0.03 N/m at room temperature. An arbitrary-waveform generator (Agilent 33220A) was used to supply the dc voltage, which was imposed between the needle-array template and ITO glass through an amplifier/controller (TREK 610E HV). The entire electrohydrodynamic patterning process was observed in real time on the contact angle platform Dataphysics (OCA20). This platform was also used to


DOI: 10.1021/acsami.6b04192
ACS Appl. Mater. Interfaces XXXX, XXX, XXX−XXX

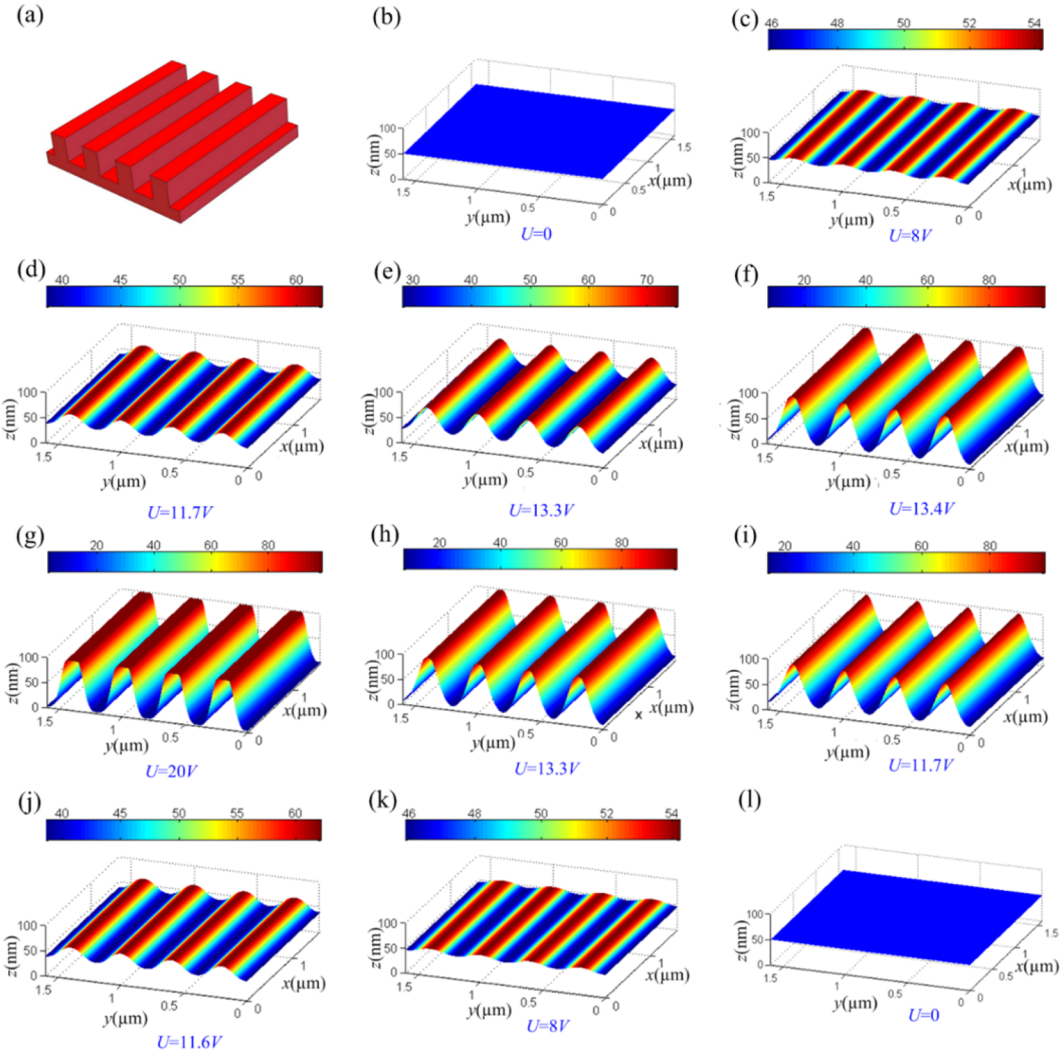


**Figure 2.** Simulation results of the electrohydrodynamic patterning for a template with periodic grooves: (a) morphology of the template; (b–l) polymer/air interface profiles under different external voltages. The voltage was increased from 0 to 20 V and then decreased back to 0 V. For each voltage, the subfigure indicates the corresponding equilibrium deformation.

measure the obtained microstructures. One important issue for the experiments is to estimate the time to achieve the equilibrium state. The following forces can be employed: the electric force $f_e \approx \varepsilon_0\varepsilon_r(U/d_0)^2$ and the viscous force $f_v \approx \mu u/d_0$. Balancing these two forces, the velocity can be obtained, $u \approx \varepsilon_0\varepsilon_r U^2/(\mu d_0)$, and the time scale is approximately $t \approx d_0/u \approx \mu {d_0}^2/(\varepsilon_0\varepsilon_r U^2)$. For the given polymer material and a voltage of 1 V, the time scale is 1 min. Thus, a few hours is long enough to ensure the equilibrium state.

## RESULTS AND DISCUSSION

Employing the aforementioned numerical model, the equilibrium state of electrohydrodynamic patterning could be obtained for different templates. In what follows, the equilibrium states are discussed for the periodic groove template, block pattern template, and needle-array template, with special interest focused on the hysteresis phenomenon, which, by the way, occurs in some other nonlinear systems.[42]

**Template with Periodic Grooves.** The template with periodic grooves is studied first, and is one of the most commonly used templates in experiments (see Figure 2a for the template morphology). An external voltage was imposed between the electrode pair. As a response the polymer film starts to deform due to the electric force. Eventually an equilibrium state is obtained for the given voltage. For convenience, a set of default parameter values are specified and listed in Table 1. These values will remain the same in the following sections unless otherwise indicated. For the given parameters, the equilibrium polymer film deformations under different voltages are exhibited in Figure 2b–l. During the

**Table 1. Constants and Parameters Used in the Simulations**

| parameter | value |
|---|---|
| free space electric permittivity ($\varepsilon_0$) | $8.85 \times 10^{-12}$ F/m |
| dielectric constant of air ($\varepsilon_1$) | 1 |
| dielectric constant of the polymer ($\varepsilon_2$) | 5 |
| interfacial tension coefficient ($\gamma$) | 30 mN/m |
| thickness of the polymer ($h_0$) | 50 nm |
| periodic length of the template ($\lambda$) | 400 nm |
| distance between two electrodes ($d_0$) | 100 nm |
| structure height on the template ($\Delta L$) | 50 nm |
| line/spacing ratio of the template | 1 |
| effective Hamaker constant for the upper electrode ($A_U$) | $10^{-20}$ J |
| effective Hamaker constant for the lower electrode ($A_L$) | $10^{-20}$ J |


DOI: 10.1021/acsami.6b04192
ACS Appl. Mater. Interfaces XXXX, XXX, XXX−XXX

process of electrohydrodynamic patterning, the bottom of the polymer film always keep contact with the ITO glass, and only the polymer/air interface is depicted in the figure to indicate the deformation of the film. We begin with a zero voltage and a flat polymer/air interface as the starting state. For such a zero voltage case, the flat interface is the equilibrium state as no surface tension force is needed to balance the electric force (see Figure 2b). After a small value voltage is imposed, some ripples appear on the polymer film (see Figure 2c), and each ripple precisely corresponds to one protrusion on the template. This is understandable as the deformation of the polymer film is caused by the nonuniform electric force on the interface, and this force is modulated by the template structure. To be specific, the protrusion on the template corresponds to a large value of the electric force, and the groove part to the small one. With an increase of the voltage, the deformed ripple becomes pronounced (see Figure 2d,e) owing to the increased electric force along the interface. The system achieves a critical state when the voltage $U$ = 13.3 V, for which a small increase in the voltage causes the polymer to grow dramatically until it is impeded by the template constraint. By comparing parts e and f of Figure 2, one can see the corresponding equilibrium deformation differs remarkably when the voltage is increased by 0.1 V. Such a value $U$ = 13.3 V is defined as the critical voltage above which the polymer film evolves to "contact" the template.

If the voltage is further increased, the polymer starts to spread along the bottom of the template (Figure 2g). The polymer film achieves its equilibrium state where the electric force is balanced by the surface tension and the LW force. After that, we start to decrease the voltage. What is surprising is that the deformation is different from that when the voltage increases. As evidenced by Figure 2h, the polymer still "contacts" the template when the voltage decreases to $U$ = 13.3 V, which contrasts with Figure 2e. Actually, the polymer starts to "detach" from the template when the voltage is reduced to $U$ = 11.7 V (see Figure 2i,j). After that, the equilibrium deformation coincides with that in the case of increasing the voltage (Figure 2k,l).

To quantitatively represent the polymer film deformation, in this study the parameter $\Delta h$ is defined as the structure height of the deformed polymer film:

$$\Delta h = \max[h(x, y)] - \min[h(x, y)] \quad (2)$$

which represents the difference between the maximum and the minimum of the polymer film thickness; for instance, $\Delta h$ = 23.5 nm for the structure in Figure 2e. The dependence of the structure height $\Delta h$ on the applied voltage $U$ is plotted in Figure 3a with the dielectric constant $\varepsilon_2$ varying from 2 to 3, 5, and 10. Meanwhile, the maxima and minima of the polymer structure, $max[h(x, y)]$ and $min[h(x, y)]$, are also monitored and are shown in Figure 3b. We take the curves of $\varepsilon_2$ = 3, for instance; the structure height increases with the voltage (i.e., the maxima increase their values and the minima decrease accordingly). When the voltage achieves its critical value (i.e., point A), a small increase of the voltage causes the structure height to grow dramatically (see point B). The structure height vs voltage takes the path of D−A−B. By checking the maximum value in Figure 3b, one can see the polymer has "touched" the template. Further increasing the voltage leads the polymer to spread along the template, and the minimum value is further reduced owing to the requirement of mass conservation. When we reduce the voltage, the structure height however takes the

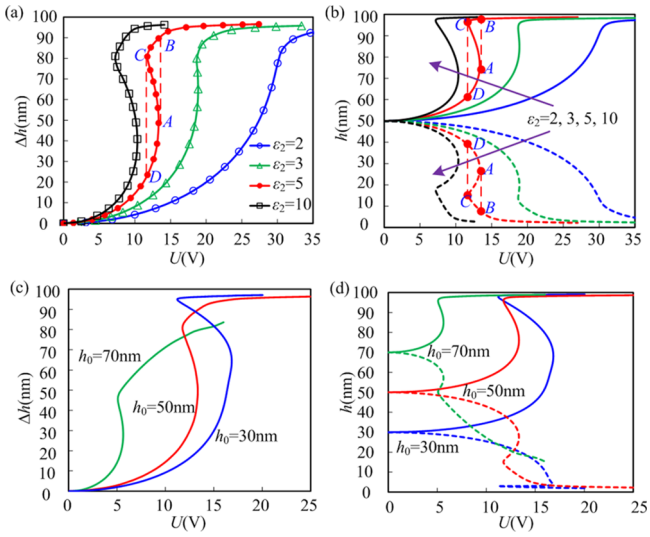


**Figure 3.** Effects of the electrical permittivity $\varepsilon_2$ and polymer film thickness $h_0$ on the hysteresis phenomenon: (a) dependency of the equilibrium structure height on the voltage for different electrical permittivities $\varepsilon_2$; (b) maxima and minima of the polymer film thickness; (c) equilibrium structure height vs external voltage for different initial film thicknesses $h_0$; (d) maximum and minimum film thickness vs voltage. The solid lines represent the maxima of the polymer film thickness and the dashed lines the minima.

route of B−C−D. This indicates that a relatively smaller voltage is needed to maintain the large structure height once the polymer grows toward the template. Such a hysteresis phenomenon as indicated by the "S"-shaped curve is caused by the nonlinear effect of electrohydrodyanmic patterning. The A−C part on the curve represents the mathematical solution to the governing eq 1; however, it is physically impossible for the system. We define point A as the first critical voltage and point C as the second critical voltage. A hysteresis phenomenon occurs when the first and second critical voltages are mismatched.

The dielectric constant $\varepsilon_2$ is a key factor in this hysteresis phenomenon as it determines the magnitude of the electric force. In Figure 3a,b, the influence of the dielectric constant on the structure height can be observed. One interesting phenomenon is that the hysteresis is enhanced by a large dielectric constant but weakened by a small dielectric constant; it even disappears for $\varepsilon_2$ = 2. After tracing the $\Delta h$−$U$ curves for different dielectric constants, we found the critical dielectric constant occurs at $\varepsilon_2$ = 2.68, where the hysteresis starts to vanish. For the curves with $\varepsilon_2$ < 2.68, the structure height is a single-value function of the voltage. However, if $\varepsilon_2$ > 2.68, $\Delta h$ is multivalued in the region between the first and second critical voltages. Take $\varepsilon_2$ = 5, for instance; three values of the structure height can be found for the same voltage. On the other hand, $\varepsilon_2$ = 2.68 is the boundary that separates these two cases. Similar behavior has been observed for a liquid droplet in an electric/magnetic field.[42,43]

Another key factor which influences the hysteresis is the polymer film thickness ($h_0$). To check this, we studied the detailed effect as plotted in Figure 3c,d. Three representative thicknesses were chosen here, i.e., 70, 50, and 30 nm. For the caseof $h_0$ = 70 nm, the polymer film is rather thick (i.e., close to the template). Thus, the "contact" with the template (i.e., the first critical voltage) occurs with a small voltage. A thick residual layer is left, and the minima of the polymer film will be further


DOI: 10.1021/acsami.6b04192
ACS Appl. Mater. Interfaces XXXX, XXX, XXX−XXX

reduced when the voltage is increased. For $h_0$ = 30 nm, the first critical voltage is high as a large electric force is necessary to "attract" the thin polymer film to the template. The case of $h_0$ = 50 nm is intermediate.

The deformation of the polymer film is essentially caused by the force imposed along the interface. As shown in Figure 4a,

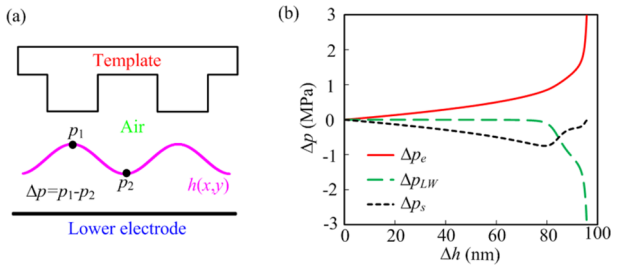


**Figure 4.** Dependence of the pressure difference on the interfacial deformation: (a) schematics of the pressure difference $\Delta p$; (b) relationship of the pressure difference $\Delta p$ with the structure height $\Delta h$. The pressure consists of three components: $p_e$ represents the pressure due to the electric force, $p_{LW}$ denotes that caused by the LW force, and $p_s$ denotes the pressure caused by the surface tension.

the pressures (i.e., the force upon unit area) at the maximum point and minimum point are denoted by $p_1$ and $p_2$ correspondingly and monitored during the deformation process. The entire force can be balanced by the gauge pressure (i.e., $P_{gag}$ in eq 1), and only the nonuniformity of the force (i.e., $\Delta p = p_1 - p_2$) determines the interfacial deformation. As analyzed in the previous section, the pressure is the summation of three components, $p = p_e + p_{LW} + p_s$, where

$$p_e = \frac{1}{2}\varepsilon_0\left(\frac{1}{\varepsilon_1} - \frac{1}{\varepsilon_2}\right)\left[\frac{\varepsilon_1\varepsilon_2 U}{\varepsilon_1 h + \varepsilon_2(d-h)}\right]^2$$

represents the pressure caused by the electric force,

$$p_{LW} = \frac{A_L}{6\pi h^3} - \frac{A_U}{6\pi(d-h)^3}$$

the pressure due to the LW force, and $p_s = \gamma\nabla^2 h$ the pressure caused by the surface tension. The pressure differences for these three components at the two points (i.e., 1 and 2 in Figure 4a) are depicted in Figure 4b for different structure heights $\Delta h$. The dielectric constant is set as $\varepsilon_2$ = 5 and the polymer film thickness as $h_0$ = 50 nm. As evidenced in the figure, the electric force tends to deform the polymer film, and this effect gets stronger with the structure height. On the other hand, the surface tension hinders the deformation and counterbalances the electric force. The surface tension first increases with the deformation but then decreases with the structure height. The reason lies in that the polymer film becomes flattened at points 1 and 2 once it gets significantly deformed and "contacts" the template and substrate. The surface tension at point 1 and point 2 can be neglected in this circumstance. As for the LW force, it closely depends on the distance between the polymer/air interface and the template and substrate. This force is ignorable for a small deformation as the interface is close to neither the template nor the substrate. However, it becomes significant and is responsible for balancing the electric force when the deformation is large.

**Template with Block Patterns.** Now we turn our attention to the template with block patterns, which is another frequently encountered template in experiments. Figure 5a illustrates such a template, and parts b–j of Figure 5 give the computational results of polymer/air interfacial deformation under different voltages. As shown in Figure 5b, the interface is ideally flat when $U$ = 0. The reason is as stated before. When the voltage increases, the interface begins to deform due to the action of the electric force; some "pine"-like patterns can be observed when $U$ = 11.9 V (see Figure 5c). Like the case of the periodic-groove template, a critical voltage ($U$ = 12.8 V) is observed as evidenced by Figure 5d,e. For a voltage higher than this critical value, the top surface of the polymer structure becomes "flat" as it has contacted the bottom of the template. In such a case, the polymer structure "bridges" the substrate and the template. A pillar array is formed, as can be seen in Figure 5e,f. When the voltage is increased, a hysteresis phenomenon also occurs in this case. The second critical voltage corresponding to the polymer detaching from the template is $U$ = 11.9 V, which is different from the first critical voltage ($U$ = 12.8 V). After detaching from the template, the polymer film falls down with a further decrease of the voltage. It returns to a flat surface when $U$ = 0.

For a better view of the hysteresis phenomenon, the structure height and the maxima and minima of the structure are plotted in Figure 5k,l. As can be seen, the curves are similar to those in the periodic-groove template case. The curve takes the D–A–B path when the voltage is increased and follows the route B–C–A when the voltage is decreased. Such an "S"-shaped curve indicates the hysteresis also occurs for the block template.

**Template with a Needle Array.** The metal needles are highly conductive and tapered at the tips (usually microscale); thus, an array of needles can be used as an economic template. Utilizing such a template, we conducted experiments of electrohydrodynamic patterning. An external electric field was imposed between the needle-array template and the ITO glass, which triggers the entire process.

This voltage was maintained for a couple of hours to guarantee the polymer film achieved its equilibrium state. Then we changed the voltage value and repeated the above procedure. The equilibrium deformation under different voltages was monitored, and the results are shown in Figure 6. As can be seen, the polymer film is flat when the voltage is zero, and then the deformation emerges with an increase of the voltage (see Figure 6b). If the voltage is further increased, the polymer film comes into contact with the template (see Figure 6c). The reason we show the result of $U$ = 389 V is that it is the first critical voltage at which the polymer film contacts the template. Then we decrease the voltage; however, the polymer remains attached to the template until $U$ = 150 V. After detaching from the template, the polymer film recedes to be flat if the voltage is switched off. The above observations demonstrate the hysteresis takes place in the experiments.

For the case shown in Figure 6, the distance between two adjacent needles is a key parameter for the structure formation. A large distance is needed for a faithful replication; i.e., one structure on the template corresponds to one pattern on the polymer film. Otherwise, for a small needle–needle distance, the structures on the film tend to coalesce together due to the interaction of the two adjacent needles.[44] In the experiments, the needle–needle distance is set as 120 $\mu$m, which has been demonstrated to be large enough for the given parameters in Table 2.


DOI: 10.1021/acsami.6b04192
ACS Appl. Mater. Interfaces XXXX, XXX, XXX–XXX

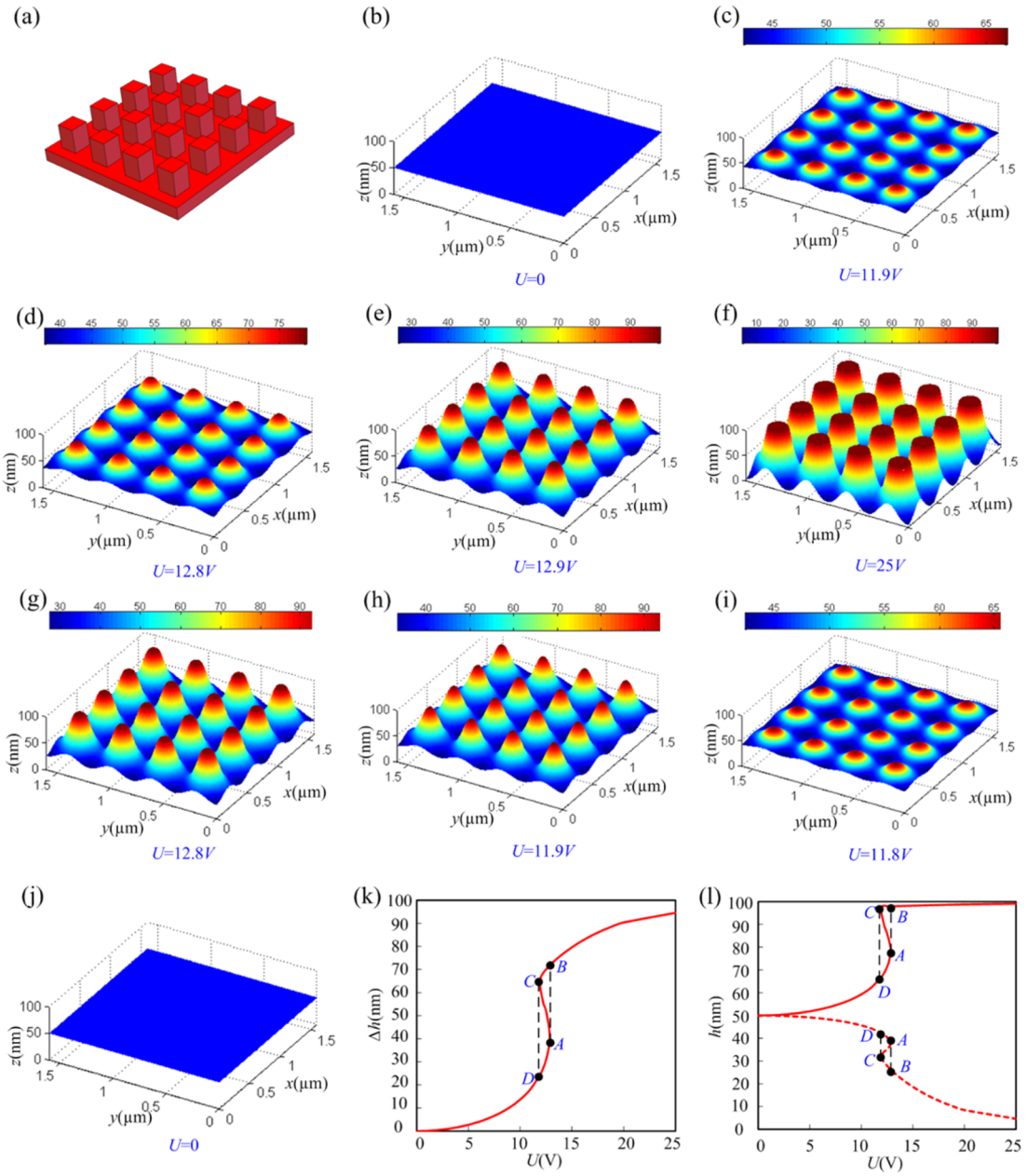


**Figure 5.** Simulation results of the electrohydrodynamic patterning for a template with a block matrix: (a) morphology of the template; (b–j) interfacial morphology for different voltages (the voltage started from 0 and rose to 25 V; then it was decreased back to 0); (k) relationship between the equilibrium structure height $\Delta h$ and the imposed external voltage $U$; (l) maxima and minima of the film thickness vs the voltage.

Numerical simulations for the needle-array template were also carried out. With the parameters listed in Table 2, the obtained results are illustrated in Figure 7. Parts a–h of Figure 7 show the interfacial morphology for different voltage values, and Figure 7i shows the dependency of the structure height on the applied voltage. Similar to the other shaped templates, a hysteresis phenomenon can be observed. This could lead us to conclude that the hysteresis phenomenon commonly occurs for different templates in electrohydrodynamic patterning.

## CONCLUDING REMARKS

A finite difference method enhanced with an arc length continuation algorithm is developed to investigate the equilibrium state of electrohydrodynamic patterning. Three representative templates, the periodic-groove template, block-patterned template, and needle-array template, are studied. It is found that a hysteresis phenomenon exists in the relationship of the voltage and structure height. A large voltage is needed to "induce" the polymer to grow toward the template, while a relatively smaller voltage is sufficient to maintain the structure height once the polymer film comes into contact with the template. Such a phenomenon is experimentally observed for the needle-array template. The effect of the parameters on the hysteresis phenomenon is also studied. It is found that the hysteresis is significantly affected by the dielectric constant. It disappears when the dielectric constant is small. The findings in this paper are of importance for the micro/nanofabrication via electrohydrodynamic patterning.


DOI: 10.1021/acsami.6b04192
ACS Appl. Mater. Interfaces XXXX, XXX, XXX–XXX

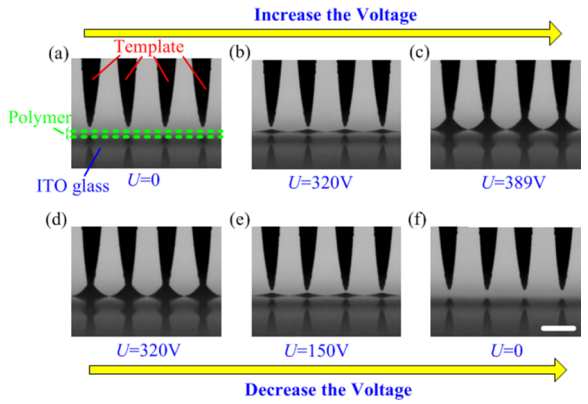


**Figure 6.** Experimental observations of the electrohydrodynamic patterning. An external voltage was applied between the needle-array electrode and ITO glass. The voltage was increased from 0 to 389 V (a–c) and then decreased back to 0 (d–f). Each value of the voltage was maintained for a few hours to ensure the interface deformation was in its equilibrium state. The electric field can be estimated by dividing the voltage by the distance between the two electrodes (i.e., $d_0$). By this means, the electric fields, from (a) to (f), are 0, $6.4 \times 10^6$, $7.8 \times 10^6$, $6.4 \times 10^6$, $3.0 \times 10^6$, and 0 V/m, correspondingly. The scale bar represents 100 $\mu$m.

**Table 2. Parameters Used for the Needle-Array Template**

| parameter | value |
|---|---|
| free space electric permittivity ($\varepsilon_0$) | $8.85 \times 10^{-12}$ F/m |
| dielectric constant of air ($\varepsilon_1$) | 1 |
| dielectric constant of the polymer ($\varepsilon_2$) | 6 |
| interfacial tension coefficient ($\gamma$) | 30 mN/m |
| thickness of the polymer ($h_0$) | 20 $\mu$m |
| periodic length of the template ($\lambda$) | 120 $\mu$m |
| distance between two electrodes ($d_0$) | 50 $\mu$m |
| effective Hamaker constant for the upper electrode ($A_U$) | $10^{-20}$ J |
| effective Hamaker constant for the lower electrode ($A_L$) | $10^{-20}$ J |

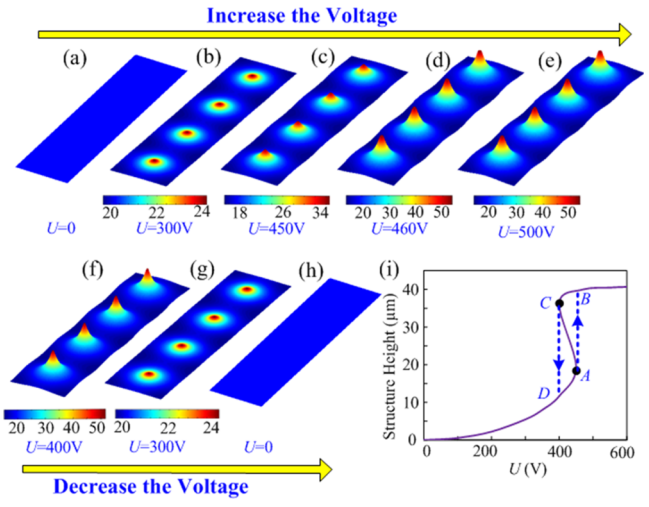


**Figure 7.** Simulation results of the electrohydrodynamic patterning for a needle-array template: (a–h) equilibrium interfacial morphology under different voltages (the voltage was first increased from 0 to 500 V and then decreased back to 0; during this process, the equilibrium deformation was captured); (i) equilibrium structure height vs applied voltage.

## ASSOCIATED CONTENT

### Supporting Information

The Supporting Information is available free of charge on the ACS Publications website at DOI: 10.1021/acsami.6b04192.

Details of the numerical model and the associated computational methodology (PDF)

## AUTHOR INFORMATION

### Corresponding Author

*E-mail: fengxu@mail.xjtu.edu.cn.

### Notes

The authors declare no competing financial interest.

## ACKNOWLEDGMENTS

This work was financially supported by the National Natural Science Foundation of China (Grants 11372243, 11532009, and 11522219), the China Postdoctoral Science Foundation (Grant 2015M570826), the Fundamental Research Funds for the Central Universities (Grant xjj2016074), the National Engineering Laboratory for Highway Maintenance Equipment (Chang'an University) (Grant 310825161103), and the Foundation of Shaanxi Postdoctoral Science.

## REFERENCES

(1) Khim, D. Y.; Han, H.; Baeg, K. J.; Kim, J. W.; Kwak, S. W.; Kim, D. Y.; Noh, Y. Y. Simple Bar-Coating Process for Large-Area, High-Performance Organic Field-Effect Transistors and Ambipolar Complementary Integrated Circuits. *Adv. Mater.* **2013**, *25* (31), 4302–4308.

(2) Yan, W. B.; Kim, J. Y.; Xing, W. D.; Donavan, K. C.; Ayvazian, T.; Penner, R. M. Lithographically Patterned Gold/Manganese Dioxide Core/Shell Nanowires for High Capacity, High Rate, and High Cyclability Hybrid Electrical Energy Storage. *Chem. Mater.* **2012**, *24* (12), 2382–2390.

(3) Duan, H. G.; Hu, H. L.; Kumar, K.; Shen, Z. X.; Yang, J. K. W. Direct and Reliable Patterning of Plasmonic Nanostructures with Sub-10-nm Gaps. *ACS Nano* **2011**, *5* (9), 7593–7600.

(4) Gatzen, H. H.; Saile, V.; Leuthold, J. *Micro and Nano Fabrication*; Springer: New York, 2015.

(5) Wu, N.; Russel, W. B. Micro- and Nano-Patterns Created via Electrohydrodynamic Instabilities. *Nano Today* **2009**, *4* (2), 180–192.

(6) Lei, X. Y.; Wu, L.; Deshpande, P.; Yu, Z. N.; Wu, W.; Ge, H. X.; Chou, S. Y. 100 nm Period Gratings Produced by Lithographically Induced Self-Construction. *Nanotechnology* **2003**, *14* (7), 786–790.

(7) Chou, S. Y.; Zhuang, L. Lithographically induced Self-Assembly of Periodic Polymer Micropillar Arrays. *J. Vac. Sci. Technol., B: Microelectron. Process. Phenom.* **1999**, *17* (6), 3197–3202.

(8) Chou, S. Y.; Zhuang, L.; Guo, L. J. Lithographically Induced Self-Construction of Polymer Microstructures for Resistless Patterning. *Appl. Phys. Lett.* **1999**, *75* (7), 1004–1006.

(9) Schaffer, E.; Thurn-Albrecht, T.; Russell, T. P.; Steiner, U. Electrically Induced Structure Formation and Pattern Transfer. *Nature* **2000**, *403* (6772), 874–877.

(10) Atta, A.; Crawford, D. G.; Koch, C. R.; Bhattacharjee, S. Influence of Electrostatic and Chemical Heterogeneity on the Electric-Field-Induced Destabilization of Thin Liquid Films. *Langmuir* **2011**, *27* (20), 12472–12485.

(11) Li, X. M.; Tian, H. M.; Ding, Y. C.; Shao, J. Y.; Wei, Y. P. Electrically Templated Dewetting of a UV-Curable Prepolymer Film for the Fabrication of a Concave Microlens Array with Well-Defined Curvature. *ACS Appl. Mater. Interfaces* **2013**, *5* (20), 9975–9982.

(12) Jiang, L.; Zhao, Y.; Zhai, J. A Lotus-leaf-like Superhydrophobic Surface: A Porous Microsphere/Nanofiber Composite Film Prepared by Electrohydrodynamics. *Angew. Chem., Int. Ed.* **2004**, *43* (33), 4338–4341.



DOI: 10.1021/acsami.6b04192
*ACS Appl. Mater. Interfaces* XXXX, XXX, XXX–XXX

(13) Hu, H.; Tian, H. M.; Li, X. M.; Shao, J. Y.; Ding, Y. C.; Liu, H. Z.; An, N. L. Biomimetic Mushroom-Shaped Microfibers for Dry Adhesives by Electrically Induced Polymer Deformation. *ACS Appl. Mater. Interfaces* **2014**, *6* (16), 14167−14173.
(14) Lin, Z. Q.; Kerle, T.; Baker, S. M.; Hoagland, D. A.; Schaffer, E.; Steiner, U.; Russell, T. P. Electric Field Induced Instabilities at Liquid/Liquid Interfaces. *J. Chem. Phys.* **2001**, *114* (5), 2377−2381.
(15) Lin, Z. Q.; Kerle, T.; Russell, T. P.; Schaffer, E.; Steiner, U. Structure Formation at the Interface of Liquid Liquid Bilayer in Electric Field. *Macromolecules* **2002**, *35* (10), 3971−3976.
(16) Morariu, M. D.; Voicu, N. E.; Schaffer, E.; Lin, Z. Q.; Russell, T. P.; Steiner, U. Hierarchical Structure Formation and Pattern Replication Induced by an Electric Field. *Nat. Mater.* **2003**, *2* (1), 48−52.
(17) Leach, K. A.; Gupta, S.; Dickey, M. D.; Willson, C. G.; Russell, T. P. Electric Field and Dewetting Induced Hierarchical Structure Formation in Polymer/Polymer/Air Trilayers. *Chaos* **2005**, *15* (4), 047506.
(18) Tian, H. M.; Wang, C. H.; Shao, J. Y.; Ding, Y. C.; Li, X. M. Electrohydrodynamic Pressure Enhanced by Free Space Charge for Electrically Induced Structure Formation with High Aspect Ratio. *Langmuir* **2014**, *30* (42), 12654−12663.
(19) Tian, H. M.; Shao, J. Y.; Ding, Y. C.; Li, X. M.; Hu, H. Electrohydrodynamic Micro-/Nanostructuring Processes Based on Prepatterned Polymer and Prepatterned Template. *Macromolecules* **2014**, *47* (4), 1433−1438.
(20) Pease, L. F.; Russel, W. B. Linear Stability Analysis of Thin Leaky Dielectric Films Subjected to Electric Fields. *J. Non-Newtonian Fluid Mech.* **2002**, *102* (2), 233−250.
(21) Wu, X. F.; Dzenis, Y. A. Electrohydrodynamic Instability of Thin Conductive Liquid Films. *J. Phys. D: Appl. Phys.* **2005**, *38* (16), 2848−2850.
(22) Gambhire, P.; Thaokar, R. M. Role of Conductivity in the Electrohydrodynamic Patterning of Air-Liquid Interfaces. *Phys. Rev. E* **2012**, *86* (3), 036301.
(23) Deshpande, P.; Chou, S. Y. Lithographically Induced Self-Assembly of Microstructures with a Liquid-Filled Gap Between the Mask and Polymer Surface. *J. Vac. Sci. Technol., B: Microelectron. Process. Phenom.* **2001**, *19* (6), 2741−2744.
(24) Gambhire, P.; Thaokar, R. Electrokinetic Model for Electric-Field-Induced Interfacial Instabilities. *Phys. Rev. E* **2014**, *89* (3), 032409.
(25) Reddy, P. D. S.; Bandyopadhyay, D.; Sharma, A. Self-Organized Ordered Arrays of Core-Shell Columns in Viscous Bilayers Formed by Spatially Varying Electric Fields. *J. Phys. Chem. C* **2010**, *114* (49), 21020−21028.
(26) Wu, L.; Chou, S. Y. Dynamic Modeling and Scaling of Nanostructure Formation in the Lithographically Induced Self-Assembly and Self-Construction. *Appl. Phys. Lett.* **2003**, *82* (19), 3200−3202.
(27) Verma, R.; Sharma, A.; Kargupta, K.; Bhaumik, J. Electric Field Induced Instability and Pattern Formation in Thin Liquid Films. *Langmuir* **2005**, *21* (8), 3710−3721.
(28) Nazaripoor, H.; Koch, C. R.; Sadrzadeh, M.; Bhattacharjee, S. Electrohydrodynamic Patterning of Ultra-Thin Ionic Liquid Films. *Soft Matter* **2015**, *11* (11), 2193−2202.
(29) Wu, N.; Pease, L. F.; Russel, W. B. Electric-Field-Induced Patterns in Thin Polymer Films: Weakly Nonlinear and Fully Nonlinear Evolution. *Langmuir* **2005**, *21* (26), 12290−12302.
(30) Tian, H. M.; Shao, J. Y.; Ding, Y. C.; Li, X.; Li, X. M. Numerical Studies of Electrically Induced Pattern Formation by Coupling Liquid Dielectrophoresis and Two-Phase Flow. *Electrophoresis* **2011**, *32* (17), 2245−2252.
(31) Yang, Q.; Li, B. Q.; Ding, Y. 3D Phase Field Modeling of Electrohydrodynamic Multiphase Flows. *Int. J. Multiphase Flow* **2013**, *57*, 1−9.
(32) Yang, Q.; Li, B. Q.; Ding, Y. Dynamic Modelling of Micro/Nano-Patterning Transfer by an Electric Field. *RSC Adv.* **2013**, *3* (46), 24658−24663.
(33) Kim, D.; Lu, W. Three-dimensional Model of Electrostatically Induced Pattern Formation in Thin Polymer Films. *Phys. Rev. B: Condens. Matter Mater. Phys.* **2006**, *73* (3), 035206.
(34) Li, H.; Yu, W.; Zhang, L.; Liu, Z.; Brown, K. E.; Abraham, E.; Cargill, S.; Tonry, C.; Patel, M. K.; Bailey, C.; Desmulliez, M. P. Y. Simulation and Modelling of Sub-30 nm Polymeric Channels Fabricated by Electrostatic Induced Lithography. *RSC Adv.* **2013**, *3* (29), 11839−11845.
(35) Tian, H. M.; Shao, J. Y.; Ding, Y. C.; Li, X.; Li, X. M.; Liu, H. Z. Influence of Distorted Electric Field Distribution on Microstructure Formation in the Electrohydrodynamic Patterning Process. *J. Vac. Sci. Technol. B* **2011**, *29* (4), 041606.
(36) Tian, H. M.; Shao, J. Y.; Ding, Y. C.; Li, X. M.; Liu, H. Z. Simulation of Polymer Rheology in an Electrically Induced Micro- or Nano-Structuring Process Based on Electrohydrodynamics and Conservative Level Set Method. *RSC Adv.* **2014**, *4* (42), 21672−21680.
(37) Yang, Q.; Li, B. Q.; Ding, Y. A Numerical Study of Nanoscale Electrohydrodynamic Patterning in a Liquid Film. *Soft Matter* **2013**, *9* (12), 3412−3423.
(38) Yang, Q.; Li, B. Q.; Ding, Y.; Shao, J. Steady State of Electrohydrodynamic Patterning of Micro/Nanostructures on Thin Polymer Films. *Ind. Eng. Chem. Res.* **2014**, *53* (32), 12720−12728.
(39) Heier, J.; Groenewold, J.; Steiner, U. Pattern Formation in Thin Polymer Films by Spatially Modulated Electric Fields. *Soft Matter* **2009**, *5* (20), 3997−4005.
(40) Yeoh, H. K.; Xu, Q.; Basaran, O. A. Equilibrium Shapes and Stability of a Liquid Film Subjected to a Nonuniform Electric Field. *Phys. Fluids* **2007**, *19* (11), 114111.
(41) Wu, N.; Russel, W. B. Dynamics of the Formation of Polymeric Microstructures Induced by Electrohydrodynamic Instability. *Appl. Phys. Lett.* **2005**, *86* (24), 241912.
(42) Sherwood, J. D. Breakup of Fluid Droplets in Electric and Magnetic-Fields. *J. Fluid Mech.* **1988**, *188*, 133−146.
(43) Behjatian, A.; Esmaeeli, A. Equilibrium Shape and Hysteresis Behavior of Liquid Jets in Transverse Electric Fields. *J. Electrost.* **2015**, *75*, 5−13.
(44) Tian, H.; Ding, Y.; Shao, J.; Li, X.; Liu, H. Formation of Irregular Micro-or Nano-Structure with Features of Varying Size by Spatial Fine-Modulation of Electric Field. *Soft Matter* **2013**, *9* (33), 8033−8040.


DOI: 10.1021/acsami.6b04192
*ACS Appl. Mater. Interfaces* XXXX, XXX, XXX−XXX